

Fabrication and Investigation of the Magnetic Properties of Co and Co₃O₄ Nanoparticles

Fardin Taghizadeh

Department of Physics, College of Sciences, Yasouj University, Yasouj, Iran
Email: taghizadeh@yu.ac.ir

Received 19 May 2016; accepted 18 August 2016; published 25 August 2016

Abstract

The nanoparticles exhibit some novel optical and magnetic properties, which are different from its bulk material. Cobalt oxide has been known as a semi-conductor compound of p type with a Spinel structure. Therefore, they are used as gas sensor and absorbent of solar energy. Furthermore, they are employed as an effective catalyzer in environmental clearing. In the thermal gradation method, carbonyl cobalt Co₂(CO)₈ is often used as a precursor, though cobalt carbonyl is very toxic and expensive. Magnetic compounds have been among interesting issues for human beings for over 4000 years. In large societies, magnetic compounds including computer disks, credit cards, speakers, coolers, automatic doors, and many other devices can be observed on a daily basis. The structure and morphology of as-prepared Co₃O₄ nanoparticles were characterized by X-ray diffraction (XRD), transmission electron microscopy (TEM) and vibrating sample magnetometer (VSM). The TEM images showed that the product nanoparticles consisted of dispersive quasi-spherical particles with a narrow size distribution ranged from 5 to 15 nm and an average size around 10 nm. The magnetic measurements confirmed that the Co₃O₄ nanoparticles show a little ferromagnetic behavior which could be attributed to the uncompensated surface spins and finite size effects. The ferromagnetic order of the Co₃O₄ nanoparticles is raised with increasing the decomposition temperature.

Keywords

Magnetic Properties, Nano Particles, Fabrication Method, Co₃O₄

1. Introduction

In recent years, metal cobalt (Co) and cobalt oxide (Co₃O₄) have attracted a great deal of attention thanks to their special properties. Based on these special properties, they have a wide range of applications including sensors, the components of information storage, catalyzers, etc. [1] [2]. Cobalt oxide has been known as a semi-conductor compound of p type with a Spinel structure. Therefore, they are used as gas sensor and absorbent of solar energy. Furthermore, they are employed as an effective catalyze in environmental clearing [3]-[6]. Metal cobalt is important owing to its various crystal structures (fcc, hcp, ε), the type of the structure of cobalt affects its

magnetic and electronic properties [7]. The important point in fabrication of pure metals is their stability against oxidation. This is because as the size of particles declines, their resistance to oxidation diminishes as well. Recently, walked into particles have been prepared by some methods including thermal degradation [7] [8], vapor condensation [9] [10], decreased salt of cobalt [11] [12], and deposition method [13].

In the thermal gradation method, carbonyl cobalt $\text{Co}_2(\text{CO})_8$ is often used as a precursor, though cobalt carbonyl is very toxic and expensive. Recently, Shao et al conducted thermal degradation using cobalt acetate with cobalt nanoparticles of 8 - 200 nm [14]. Similarly, Lee et al have prepared cobalt nanoparticles through thermolysis of Co^{2+} -Oleat₂ [15]. In order to prevent clotting of the particles, organic surfactants are used [7]. Triphenyl phosphine (TPP) is widely used for stabilizing gold nanoparticles and other metals [16]. The phenyl groups in TPP develop more spatial disturbance than chain alkyl groups [17].

2. Method of Fabrication

In materials science, the sol-gel process is a method for producing solid materials from small molecules (**Figure 1**). The method is used for the fabrication of metal oxides, especially the oxide of cobalt.

The process involves conversion of monomers into a colloidal solution (sol) that acts as the precursor for an integrated network (or gel) of either discrete particles or network polymers. In this method, metal nanoparticles and the metal oxide have been prepared through thermal degradation of the metal-surfactant complex in a hot surfactant solution. This method is schematically shown in **Figure 2**, demonstrating the fabrication of cobalt nanoparticles.

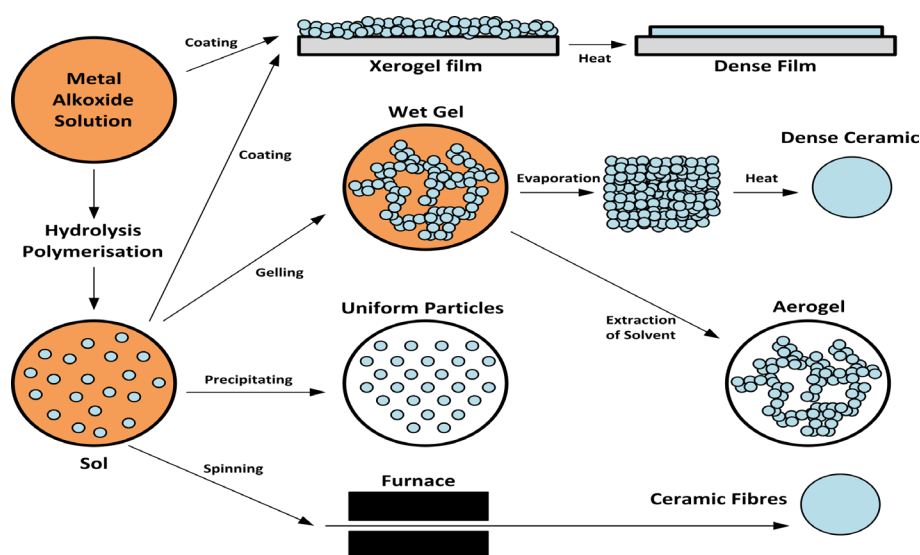


Figure 1. The sol-gel method for fabrication of nanoparticles.

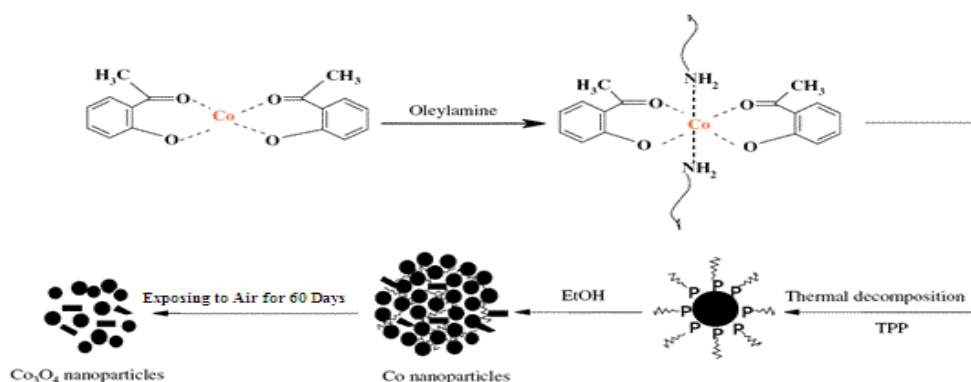


Figure 2. The procedure of fabrication of Co_3O_4 nanoparticles.

3. Magnetic Properties

Firstly, the magnetic properties and hysteresis loops of magnetic compounds are generally discussed, followed by investigation of the properties of cobalt and cobalt oxide nanoparticles.

Magnetic compounds have been among interesting issues for human beings for over 4000 years. In large societies, magnetic compounds including computer disks, credit cards, speakers, coolers, automatic doors, and many other devices can be observed on a daily basis [18].

There are various magnetic compounds including diamagnetic, paramagnetic, and ferromagnetic. Further, ferromagnetic itself is categorized into two smaller groups called anti-ferromagnetic and ferrimagnetic. When magnetic moments are positioned randomly in relation to each other, the pure magnetic moments of the Crystal is zero. This state is called paramagnetic. However, the ferromagnetic crystal has a pure magnetic moment. The ferrimagnetic crystal also has a pure magnetic moments, but magnetic areas are positioned at opposite directions to each other. One of the areas is larger than the other and thus eventually a net magnetic moment will be present. However, in the antiferromagnetic crystal, the magnetic areas are absolutely of the same size and in opposite direction. Two important properties of magnetic compounds are Curie temperature and magnetic hysteresis. Exchanged coupling and thus the Heisenberg's exchange energy are directly related to Curie temperature (T_c) of ferro and ferrimagnetic compounds. At temperatures lower than T_c , the magnetic moment is the same as the specific crystallographic direction of the zero axis of these compounds. It is preferred that this axis be called easy axis of magnetic crystal. This axis is developed in response to pairing this electron spin and the angular momentum of electron orbital. Due to presence of the easy axis, by applying an external magnetic field, the formation of the crystal of the compounds is controlled. When the magnetic field with the crystal's easy axis and its direction towards the external magnetic field overcome the barrier energy between the magnetic areas, it changes their direction towards the magnetic field. This barrier energy is known as Magnetocrystalline Anisotropy, the atomic region of the magnetic hysteresis behavior of magnetic compounds. E_A is one of the most important principles of the magnetic properties of compounds, determining the stability of compounds for special uses [18].

Ferromagnetic compounds are of interest based on their applications. Their properties should be identified quantitatively using the hysteresis loop of magnetic compounds. A hysteresis loop can be measured by placing a sample in a magnetometer and the compound's response (M , σ) to the exerted magnetic field (H). Several quantities can be obtained from the hysteresis loop [19].

Magnetic saturation (M_s) or special magnetic saturation (σ_s) are the cases that show the extent of magnetization when all bipolars have been ordered in the direction of the exerted magnetic field.

The remaining magnetic (M_r) is the magnetization of the sample in a magnetic field of zero. The inhibition force (H_c) is a force of the magnetic field required for changing the remaining magnetization. The change in the field's bias (H_E) indicates the extent of displacement off the center of hysteresis loop.

Figure 3 demonstrates the magnetization curve of a ferromagnetic compound. The total changes of magnetization of the sample M has been shown in terms of the intensity of the exerted DC field (H). Initially, when the

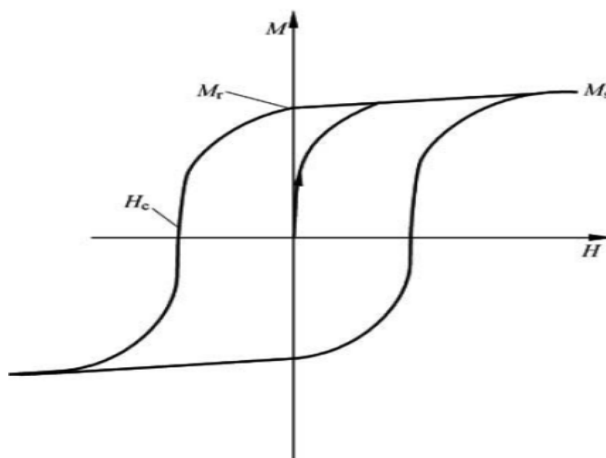


Figure 3. Hysteresis curve of a ferromagnetic.

exerted field increases, so does M , until it reaches the saturation point M_s . When the exerted field decreases from the saturation point, M does not reach its initial value, rather it stops at a point higher than the reduced field. This condition is called “residual”. It happens when the areas that have been aligned with the increase in the field do not return to their original orientation with the reduction of the field. When the exerted magnetic field H reaches zero, the magnet has still magnetization called residual magnetization (M_r). As can be seen in Figure 3, in order to remove the residual magnetization, the H_c field should be exerted in the opposite direction of the initial field. This field is called driving field, which causes the areas to rotate and return to their original positions. The properties of the magnetization curve of a ferromagnetic compound is a strong reliance for applying magnetic compounds.

Originally, the magnetic properties of compounds can be understood and controlled through magnetic pairings. Such pairings have a close relationship with the type of the chemical compound and the magnetic structure of compounds, though no accurate relationship is known between the magnetic properties of compounds, their chemical composition, and their crystal structures at an atomic level. There are various factors contributing to proper understanding of the changes of magnetic areas at atomic level by external exerted fields as well as the magnetic properties and magnetic pairings at atomic level. The structure of magnetic nanoparticles includes unique magnetic areas. Multi-area structures are not desirable in terms of energy due to their small size. Without the presence of the walls of areas, the magnetic pairing of atomic balance is directly associated with the magnetic properties of nanoparticles. Certainly, understanding and controlling the magnetic properties of nanoparticles will clarify the mechanism of magnetic properties of compounds together with its design and control. Magnetic nanoparticles are promising thanks to reduction of magnetic areas and thus development of super-paramagnetic properties. The super-paramagnetic properties of nanoparticles are directly influenced by magnetic Anisotropy of nanoparticles. As is evident in **Figure 3**, due to the symmetry of the precursor, there are sites with equal energy balances on the surface of the metal kernel. TPP is a surfactant with a high boiling point, developing a great spatial inhibition of controlling the magnetic properties of magnetic nanoparticles, despite the three phenyl groups. In addition to TPP in the mixture, presence of oleyl amine and the complexity of the precursor significantly diminish the size of particles. Oleyl amine is known as a ligand that has a suitable bond with the surface of metal nanoparticles. The combination of the effects of TPP and oleyl amine greatly contributes to development of individual nanoparticles.

4. Results and Discussion

4.1. Magnetic Results

As shown in **Figure 4** the curve exhibits an antiferromagnetic behavior. The ferromagnetic behavior of the nanoparticles can be explained as follows: bulk Co_3O_4 has a normal spinel structure with antiferromagnetic exchange between ions which occupy the tetrahedral and octahedral sites [19].

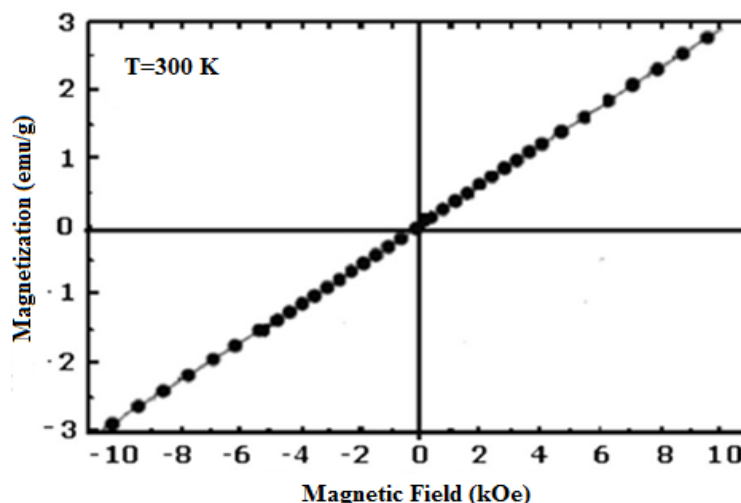


Figure 4. Compound Co_3O_4 nanoparticles [18].

The hysteresis curve for Co_3O_4 nanoparticles prepared at different temperatures were carried out at room temperature. As shown in **Figure 5** the hysteresis curve for the Co_3O_4 nanoparticles prepared at 400 K exhibits a weak ferromagnetic behavior with a saturation magnetization of $0.125 \text{ emu}\cdot\text{g}^{-1}$ at the maximum field of 9 kOe applied while the hysteresis curve for the Co_3O_4 samples prepared at 450 K and 500 K in the **Figure 6** and **Figure 7** display higher ferromagnetic properties with saturation magnetization values of 0.23 and $0.31 \text{ emu}\cdot\text{g}^{-1}$ at the applied field of 9 kOe, respectively. To confirm that the ferromagnetic behavior originates from the nanoparticles, this measurement was also conducted on a bulk sample.

The change from an antiferromagnetic state for bulk Co_3O_4 to a weakly ferromagnetic state for the Co_3O_4 nanoparticles can be ascribed to the uncompensated surface spins and finite size effects. It is well known.

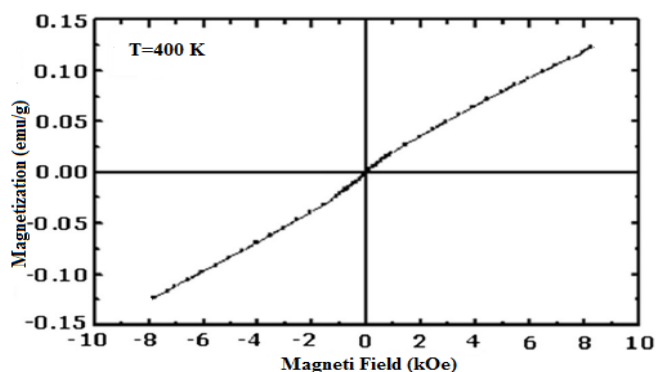


Figure 5. The hysteresis curve of Co_3O_4 nanoparticles at 400 K.

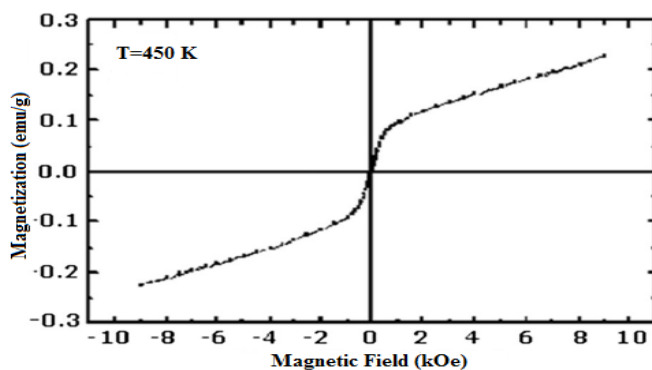


Figure 6. The hysteresis curve of Co_3O_4 nanoparticles at 450 K.

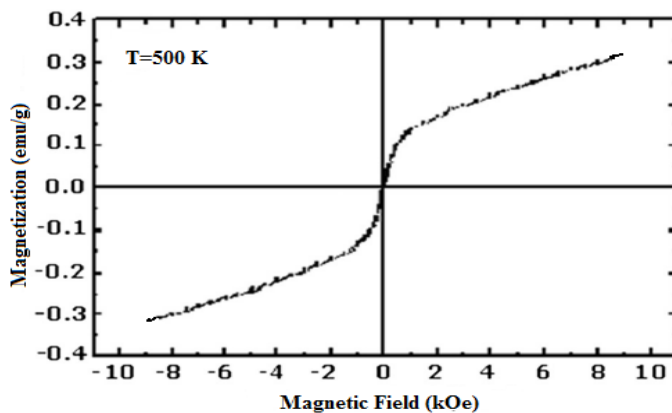


Figure 7. The hysteresis curve of Co_3O_4 nanoparticles at 500 K.

4.2. XRD Results

Figure 8 presents the X-ray Diffraction (XRD) pattern on the prepared samples. The peaks in **Figure 8** are related to 111, 200, 220, 200, and 311 planes of hcp cobalt. Due to the very small size, cobalt nanoparticles are easily oxidized when exposed to air. The XRD pattern reveals no peaks related to the cobalt oxide phase.

This is due to the protection of the surface of cobalt nanoparticles against oxidation by oleyl amine and TPP. The developed peaks are wide, attributable to the reduction in the size of particles. This shows that all cobalt particles are in nano size. It is possible to obtain the mean size of the particles by Debye-Scherrer Equation. The mean size of these samples is 20 nm. **Figure 9** demonstrates the XRD pattern of cobalt nanoparticles following exposure to air. In this figure, no peak associated with metal cobalt can be seen. The image is related to the cubic phase of Co_3O_4 with a Spinel structure. The network parameter is equal to $a = 8.085 \text{ \AA}$. No other pure peak is seen in this pattern, suggesting that the Co_3O_4 is completely pure. Separation of peaks is very good, implying that the crystal structure is single phased in the cubic crystal structure.

4.3. TEM Results

Figure 10 illustrates the TEM image of cobalt nanoparticles. The majority of Co_3O_4 nanoparticles are irregular (**Figure 10**). The mean size of Co_3O_4 nanoparticles is 10 nm. In HRTEM image (**Figure 11**), the distance be-

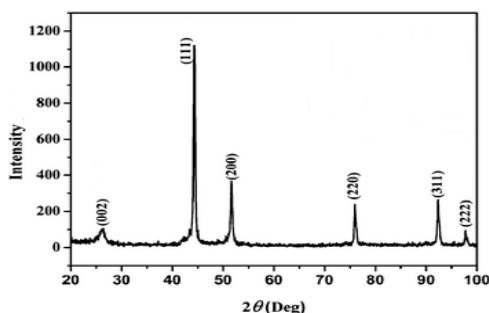


Figure 8. The XRD pattern of Co.

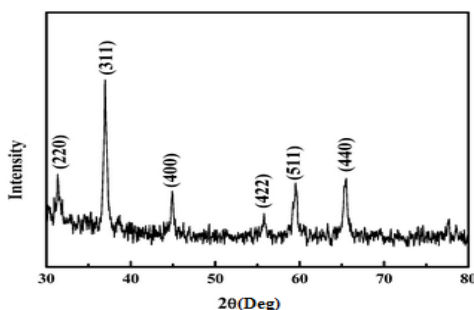


Figure 9. The XRD pattern of Co_3O_4 nanoparticles.

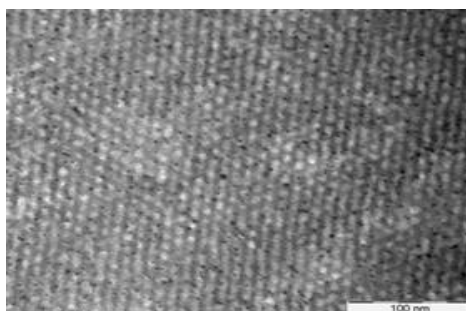


Figure 10. TEM image of Co_3O_4 nanoparticles.

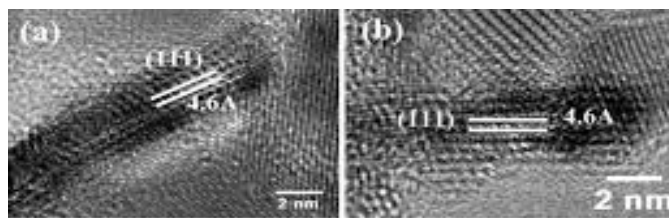


Figure 11. HRTEM image of Co_3O_4 nanoparticles.

tween the two adjacent planes (d) is 4.6 Å. The TEM images showed that the product nanoparticles consisted of dispersive quasi-spherical particles with a narrow size distribution ranged from 5 to 15 nm and an average size around 10 nm.

References

- [1] Casas-Cabanas, M., Binotto, G., Larcher, D., Lecup, A., Giordani, V. and Tarascon, J.M. (2009) Defect Chemistry and Catalytic Activity of Nanosized Co_3O_4 . *Chem Mater*, **20**, 1939-1947. <http://dx.doi.org/10.1021/cm900328g>
- [2] Askarinejad, A., Bagherzadeh, M. and Morsali, A. (2010) Catalytic Performance of Mn_2O_4 and Co_3O_4 Nanocrystals Prepared by Sonochemical Method in Epoxidation of Styrene and Cyclooctene. *Appl. Surface Sci*, **256**, 6678-6682. <http://dx.doi.org/10.1016/j.apsusc.2010.04.069>
- [3] Duan, X., Huang, Y., Agarwal, R. and Lieber, C.M. (2003) Single-Nanowire Electrically Driven Lasers. *Nature*, **421**, 241-245. <http://dx.doi.org/10.1038/nature01353>
- [4] Seo Hee, J.U., Hong, S.K. and Jang, H.C. (2007) Fine Size Cobalt Oxide Powders Prepared by Spray Pyrolysis Using Two Types of Spray Generators. *Journal of the Ceramic Society of Japan*, **115**, 507-510. <http://dx.doi.org/10.2109/jcersj2.115.507>
- [5] Lou, X.W., Deng, D., Lee, J.Y., Feng, J. and Archer L.A. (2008) Self-Supported Formation of Needlelike Co_3O_4 Nanotubes and Their Application as Lithium-Ion Battery Electrodes. *Adv Mater*, **20**, 258-262. <http://dx.doi.org/10.1002/adma.200702412>
- [6] Li, Y.G., Tan, B. and Wu, Y.Y. (2008) Mesoporous Co_3O_4 Nanowire Arrays for Lithium Ion Batteries with High Capacity and Rate Capability. *Nano Lett*, **8**, 265-270. <http://dx.doi.org/10.1021/nl0725906>
- [7] Puentes, V.F., Krishnan, K.M. and Alivisatos, A.P. (2001) Colloidal Nanocrystal Shape and Size Control: The Case of Cobalt. *Science*, **291**, 2115-2117. <http://dx.doi.org/10.1126/science.1057553>
- [8] Li, W.-Y., Xu, L.-N. and Chen, J. (2005) Co_3O_4 Nanomaterials in Lithium-Ion Batteries and Gas Sensors. *Adv Funct Mater*, **15**, 851. <http://dx.doi.org/10.1002/adfm.200400429>
- [9] Dong, H.L., Choi, C.J. and Kim, B.K. (2002) Chemical Synthesis of Co Nanoparticles by Chemical Vapor Condensation. *Scripta Mater*, **47**, 857-861. [http://dx.doi.org/10.1016/S1359-6462\(02\)00304-4](http://dx.doi.org/10.1016/S1359-6462(02)00304-4)
- [10] Makhlof, S.A. (2002) Magnetic Properties of Co_3O_4 Nanoparticles. *J Magn Magn Mater*, **246**, 184-190. [http://dx.doi.org/10.1016/S0304-8853\(02\)00050-1](http://dx.doi.org/10.1016/S0304-8853(02)00050-1)
- [11] Sun, S. and Murray, C.B. (1999) Synthesis of Monodisperse Cobalt Nanocrystals and Their Assembly into Magnetic Superlattices (Invited). *J. Appl. Phys*, **85**, 4325. <http://dx.doi.org/10.1063/1.370357>
- [12] Luna, C., Morales, M.P., Serna, C.J. and Vazquez, M. (2003) Effects of Surfactants on the Particle Morphology and Self-Organization of Co Nanocrystals. *Mater Sci Eng. C*, **23**, 1129-1132. <http://dx.doi.org/10.1016/j.msec.2003.09.165>
- [13] Sun, L., Li, H., Ren, L. and Hu, C. (2009) Synthesis of Co_3O_4 Nanostructures Using a Solvothermal Approach. *Solid State Sci*, **11**, 108-112. <http://dx.doi.org/10.1016/j.solidstatesciences.2008.05.013>
- [14] Lai, T., Lai, Y., Lee, C., Shu, Y. and Wang C. (2008) Microwave-Assisted Rapid Fabrication of Co_3O_4 Nanorods and Application to the Degradation of Phenol. *Catal Today*, **131**, 105-110. <http://dx.doi.org/10.1016/j.cattod.2007.10.039>
- [15] Lee, D.K., Kim, Y.H., Zhang, X.L. and Kang Y.S. (2006) Preparation of Monodisperse Co and Fe Nanoparticle Using Precursor of M^{2+} -Oleate₂ (M = Co, Fe). *Current Appl. Phys*, **6**, 786-790. <http://dx.doi.org/10.1016/j.cap.2005.04.040>
- [16] Yang, H.T., Su, Y.K., Shen, C.M., Yang, C.M. and Gao H.J. (2004) Synthesis and Magnetic Properties of Cobalt Nanoparticles. *Surf. Interface Anal*, **36**, 155-160. <http://dx.doi.org/10.1002/sia.1675>
- [17] Wang, R.M., Liu, C.M., Zhang, H.Z., Chen, C.P., Guo, L. and Xu, H.B. (2004) Porous Nanotubes of Co_3O_4 : Synthesis, Characterization, and Magnetic Properties. *Appl Phys Lett*, **85**, 2080. <http://dx.doi.org/10.1063/1.1789577>
- [18] Goldstein, A.N. and Dekker, M. (1997) Handbook of Nanophase Materials. *J. Am. Chem. Soc*, **120**, 4556-4556.
- [19] Wohlfarth, E.P. (1980) Ferromagnetic Materials. *Krist. Techn*, **16**, 127.



Submit or recommend next manuscript to SCIRP and we will provide best service for you:

Accepting pre-submission inquiries through Email, Facebook, LinkedIn, Twitter, etc.

A wide selection of journals (inclusive of 9 subjects, more than 200 journals)

Providing 24-hour high-quality service

User-friendly online submission system

Fair and swift peer-review system

Efficient typesetting and proofreading procedure

Display of the result of downloads and visits, as well as the number of cited articles

Maximum dissemination of your research work

Submit your manuscript at: <http://papersubmission.scirp.org/>